J. Plasma Fusion Res. SERIES, Vol. 6 (2004) 187–191

Excitation of Convective Cell Mode by Universal Drift Wave Turbulence

SAITO Tsuyoshi.[1], ITOH Sanae -I.[2], YAGI Masatoshi[2], HAHM Taik Soo[3] and CHENG Chio Z.[3]

[1]*Interdisciplinary Graduate School of Engineering Sciences Kyushu Univesity, Kasuga, 816-8580, Japan*

[2]*Research Institute for Applied Mechanics, Kyushu University Kasuga, 816-8580, Japan*

[3]*Princeton Plasma Physics Laboratory, Princeton University Princeton NJ 08543-0451, USA*

(Received: 9 December 2003 / Accepted: 6 July 2004)

Abstract

The interaction between the universal drift wave and the convective cell mode in the shearless slab geometry is investigated using a kinetic-fluid model based on nonlinear gyro-kinetic equations. It is found that the convective cell mode is nonlinearly excited in a way, which is similar to the zonal flow generation of ITG turbulence. On the other hand, if we introduce the large ion-ion collision effect, the zonal flow is damped and instead the streamer and finite k_y modes are excited in the convective cell mode. As the result, the flux is larger than that without collision. The forward cascade is observed in k_z space and the forward/inverse cascade is observed in k_y space in the time evolution of energy spectrum.

Keywords:

drift wave, convective cell, inverse cascade, zonal flow, kinetic fluid model, parametric decay instability

1. Introduction

To understand anomalous transport in high temperature plasma is a crucial issue in nuclear fusion research. ITG (ion temperature gradient driven drift wave) is a possible candidate for anomalous ion heat transport. The gyro-kinetic simulations of ITG turbulence demonstrate that zonal flows play a crucial role in regulating drift wave turbulence and the level of the anomalous transport [1]. The theoretical explanation for the generation of zonal flow is proposed based on parametric instability in shearless slab geometry [2,3]. Simulations in such a simplified drift wave system were performed long time ago[4], although parameter dependence was not examined systematically. In addition, direct comparisons of these theory to the gyro-kinetic simulation results were possible in some idealized test case only [1]. In this paper, we perform the simulation study of universal drift wave turbulence and investigate the excitation of convective cell mode in detail using a kinetic-fluid model in the shearless slab geometry. This is an extension of the models proposed by Smolyakov [5] and Hinton [6]. Our model describes the universal drift wave turbulence and nonlinear excitation of convective cell mode [3,4], which include zonal flows and streamers generated by drift waves. Simulation results show that no saturated state is attained in the universal drift wave turbulence. This is attributed to the fact instability source exists in the short wavelength region of k_y space. For ITG turbulence, the instability source exists in the long wavelength region and there is enough energy sink in the short wavelength region. These difference make it difficult to compare simulation results of universal drift wave turbulence with the theory directly, in which the linear growth rate is a given parameter and is not described self-consistently by the model itself [2]. Nevertheless, there is still an academic interest to investigate the development of universal drift wave turbulence and the excitation of convective cell mode in the three dimensional configuration space, especially in terms of cascade and inverse cascade due to not only ion nonlinearity but also electron nonlinearity, which is not included in the adiabatic electron response. This paper is organized as follows. In the next section, the Cheng-Johnson kinetic-fluid model is explained and simulation results are discussed in section **3**. The conclusions are summarized in section **4**.

2. Models

To investigate the interaction between universal drift wave and convective cell in shearless slab geometry (x, y, z) (x is the radial direction, y is the poloidal direction and z is the direction of ambient magnetic field), a kinetic-fluid model is derived integrating the nonlinear gyro-kinetic equation in the velocity space and using linear closure to reproduce the linear dispersion relation [7,8]. The ion continuity equation is written by

Corresponding author's e-mail: tsuyoshi@riam.kyushu-u.ac.jp

$$\begin{aligned}&\frac{\partial}{\partial t} n_{\boldsymbol{k}} - \mathrm{i}\omega_* \Gamma_{0k}\zeta_i Z_i \phi_{\boldsymbol{k}} + \tau(1+\Gamma_{0k}\zeta_i Z_i)\frac{\partial}{\partial t}\phi_{\boldsymbol{k}} \\ &+ \frac{\tau}{2}\sum_{\boldsymbol{k}=\boldsymbol{k}'+\boldsymbol{k}''}(\boldsymbol{b}\cdot\boldsymbol{k}''\times\boldsymbol{k}')\phi_{\boldsymbol{k}'}\chi_{\boldsymbol{k}''}(n_{\boldsymbol{k}''}+\tau\phi_{\boldsymbol{k}''}) = 0,\end{aligned} \tag{1}$$

and the electron continuity equation is by

$$\begin{aligned}&\frac{\partial}{\partial t} n_{\boldsymbol{k}} - \mathrm{i}\omega_* \zeta_e Z_e \phi_{\boldsymbol{k}} - (1+\zeta_e Z_e + k^2\lambda^2)\frac{\partial}{\partial t}\phi_{\boldsymbol{k}} \\ &+ \frac{\tau}{2}\sum_{\boldsymbol{k}=\boldsymbol{k}'+\boldsymbol{k}''}(\boldsymbol{b}\cdot\boldsymbol{k}''\times\boldsymbol{k}')\phi_{\boldsymbol{k}'}(n_{\boldsymbol{k}''}-k''2\lambda^2\phi_{\boldsymbol{k}''}) = 0,\end{aligned} \tag{2}$$

where $\boldsymbol{k}$ is the wave number vector, $n_{\boldsymbol{k}}$ is the fluctuating ion density and $\phi_{\boldsymbol{k}}$ is the electrostatic potential. $\omega_* = \tau k_y \rho_i^2/(2L_n)$ is the normalized diamagnetic drift frequency by the ion cyclotronfrequency Ω_i, where ρ_i is the ion gyro-radius, $\tau = T_e/T_i$ is the ratio of electron and ion temperature, $L_n = -(\mathrm{d}/\mathrm{d}x \ln n)^{-1}$ is the density gradient scale length. $\lambda = \sqrt{\tau}\,\Omega_i/(\sqrt{2}\,\omega_{pi})$ is the normalized Debye length by the ion Lamor radius, where ω_{pi} is the ion plasma frequency. $\Gamma_{0k} = I_0(b_k)\mathrm{e}^{-b_k}$ represents the finite Lamor effect, where I_0 is the zeroth order modified Bessel function with $b_k = k_\perp^2\rho_i^2/2$ and $k_\perp^2 = k_x^2 + k_y^2$. $Z_{i,e}$ are plasma dispersion functionwith the argument $\zeta_{i,e} = \omega/(k_z v_{i,e})$ and $\chi_{k''} = 2\int_0^\infty \mathrm{d}x x\mathrm{e}^{-x^2} J_0(b_k^{1/2}x)J_0(b_{k'}^{1/2}x)J_0(b_{k''}^{1/2}x)/\Gamma_{0k''}$, where $v_{i,e} = 2T_{i,e}/m_{i,e}$ are ion and electron thermal velocity, $T_{i,e}$ are ion and electron temperature, $m_{i,e}$ are ion and electron mass and J_0 is the zeroth order Bessel function.The factor 1/2 in eqs.(1) and (2) appears due to the definition of thermal velocity. The Poisson equation is used to eliminate the fluctuating electron density in the electron continuity equation. The energy conservation reration is obtained from eqs.(1) and (2) as

$$\begin{aligned}&\sum_{\boldsymbol{k}}\Big[\mathrm{Re}(s_2)\frac{\partial}{\partial t}\left|\phi_{\boldsymbol{k}}\right|^2 + 2\,\mathrm{Re}(s_1)\left|\phi_{\boldsymbol{k}}\right|^2 \\ &- 2\,\mathrm{Im}(s_2)\mathrm{Re}(\phi_{\boldsymbol{k}})\mathrm{Im}(\dot{\phi}_{\boldsymbol{k}}) - \mathrm{Im}(\phi_{\boldsymbol{k}})\mathrm{Re}(\dot{\phi}_{\boldsymbol{k}})\Big] = 0\end{aligned} \tag{3}$$

where $s_1 = \mathrm{i}\omega_{*e}(\zeta_e Z_e - \Gamma_{0k}\zeta_i Z_i)$, $s_2 = 1 + \zeta_e Z_e + k^2\lambda^2 + \tau(1+\Gamma_{0k}\zeta_i Z_i)$. In the fluid ion, $1 \ll \zeta_i$ and near adiabatic electron response, $\zeta_e \ll 1$, i.e., $v_i \ll \omega/k_z \ll v_e$ and neglecting the collisionless dissipations, it is reduced to $\mathrm{d}/\mathrm{d}t(E_{DW} + E_{CC}) = 0$ with

$$E_{DW} = \sum_{k_x,k_y,k_z\neq 0}\left[1 + k^2\lambda^2 + \tau(1-\Gamma_{0k})\right]\left|\phi_{\boldsymbol{k}}\right|^2,$$

$$E_{CC} = \sum_{k_x,k_y,k_z=0}\left[k^2\lambda^2 + \tau(1-\Gamma_{0k})\right]\left|\phi_{\boldsymbol{k}}\right|^2.$$

E_{DW} represents the energy of drift wave ($k_z \neq 0$) and E_{CC} represents the energy of convective cell mode ($k_z = 0$) [3,4]. In addition, the analytical dispersion relation of universal drift wave is obtained in this limit $v_i \ll \omega/k_z \ll v_e$, keeping collionless dissipations as

$$\begin{aligned}\omega = &\frac{\omega_*\Gamma_{0k}}{1+\tau(1-\Gamma_{0k})} \\ &+ \mathrm{i}\frac{(1+\tau)\omega_*\sqrt{\pi}}{[1+\tau(1-\Gamma_{0k}^2)]^2}\left[(1-\Gamma_{0k})\zeta_e\mathrm{e}^{-\zeta_e^2} - \Gamma_{0k}\zeta_i e^{-\zeta_i^2}\right]\end{aligned} \tag{4}$$

Using this model, the excitation of convective cell is investigated in the next section.

3. Simulation results

In present numerical simulations, the following parameters are used: $16\times32\times8$ Fourier modes are used in the wave number space (k_x, k_y, k_z). The smallest wave numbers are chosen as $k_{x0} = k_{y0} = 0.15$, $k_{z0} = 0.02$. The real mass ratio is used as $m_i/m_e = 1836$, then $\Omega_i^2/\omega_{pi}^2 = 10/(m_i/m_e)$. The density gradient scale length is chosen as $\rho_i/L_n = 0.2$ (the wave number is normalized by ion gyro-radius). And the effect of ion-ion collision is also investigated. The ion-ion collision is taken into account by replacing $\frac{\partial}{\partial t} \rightarrow \frac{\partial}{\partial t} + \nu_{ii}$ in the ion continuity equation, where ν_{ii} is the normalized ion-ion collision frequency by the ion cyclotron frequency. Such a simplified Krook-like collision term does not conserve particle, momentum and energy, therefore, the saturation amplitude of turbulence is not obtained accurately. However, it might be still applicable to damp the zonal flow ($k_x \neq 0, k_y = 0, k_z = 0$). In this paper, we limit our discussion on the excitation of convective cell mode in the development of turbulence not on the statistical property of turbulence in the saturation phase.

Figure 1 and 2 show dependence of the real frequency and the growth rate of universal drift wave on the wavenumber k_y. The thick line corresponds to the case with

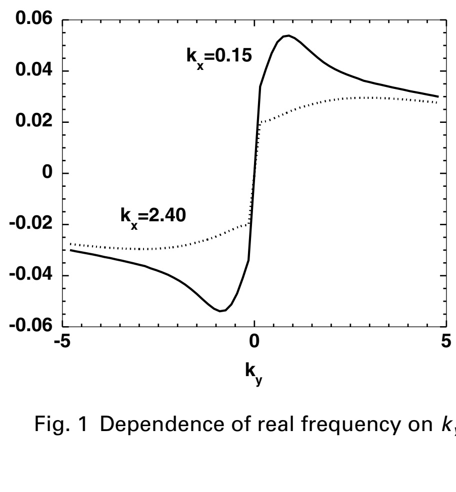

Fig. 1 Dependence of real frequency on k_y.

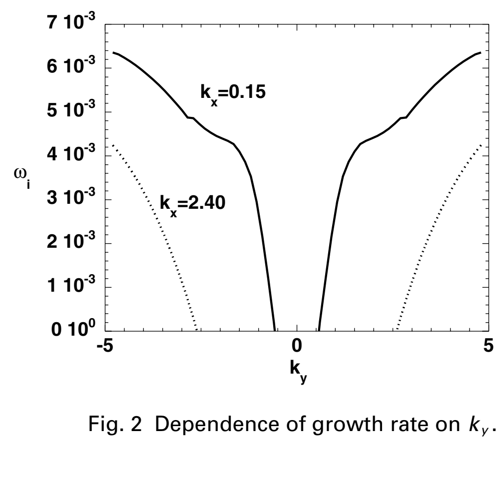

Fig. 2 Dependence of growth rate on k_y.

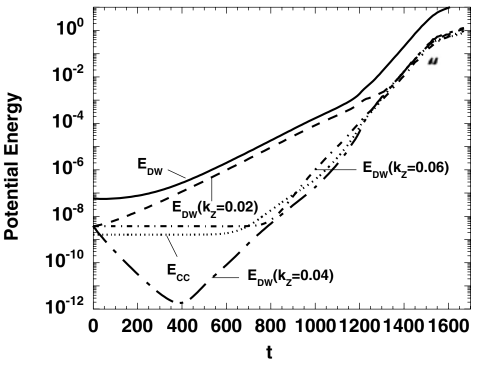

Fig. 3 Time evolution of energy for drift wave and convective cell mode.

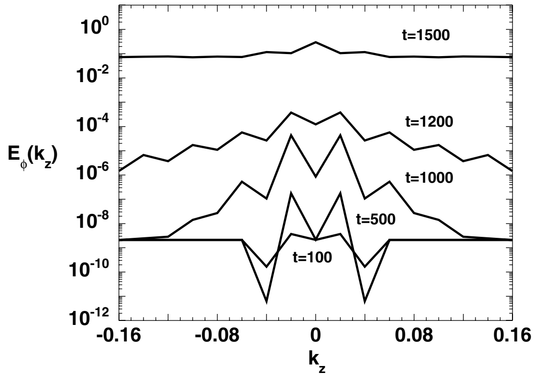

Fig. 4 Time evolution of power spectrum for potential energy $E_z(k_z)$.

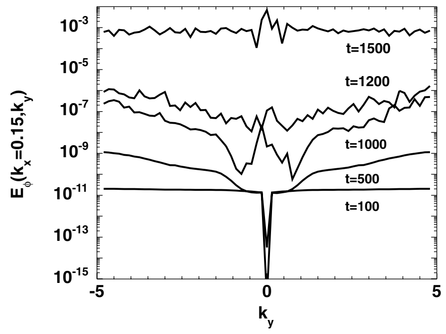

Fig. 5 Time evolution of power spectrum for potential energy $E_\phi(k_x, k_y)$ with $k_x = 0.15$.

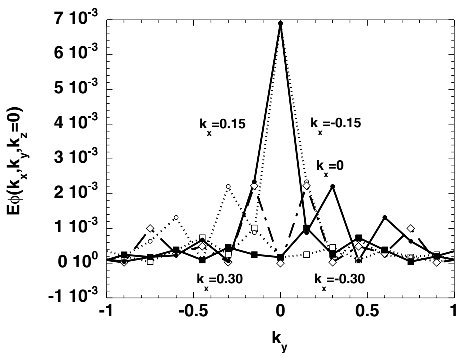

Fig. 6 Power spectrum of potential energy for convective cell mode $E_\phi(k_x, k_y, k_z = 0)$ at $t = 1500$.

$k_x = 0.15, k_z = 0.02$ and the dotted line to $k_x = 0.24$, $k_z = 0.02$, respectively. It is shown that the universal drift wave is unstable in the short wavelength region of k_y. It is found that for larger k_z, the universal drift wave is stable.

Figure 3 shows the time evolution of energy for drift wave E_{DW} and the convective cell mode E_{CC}. The thick line corresponds to the energy for drift wave and the dotted line to the energy forconvective cell mode.The energy for each Fourier mode of drift wave with $k_z = 0.02, 0.04, 0.06$ is also shown. The dashed line indicates the mode with $k_z = 0.02$, the long dashed dotted line, the mode with $k_z = 0.04$ and the short dashed dotted line, the mode with $k_z = 0.06$. The maximum growth rate of the drift wave is given by the longest wavelength mode with $k_z = \pm 0.02$. It is seen that the convective cell and the drift wave with short wavelength in k_z are nonlinearly excited. The amplitude of these modes reaches at almost the same level as $k_z = \pm 0.02$ at $t \geq 1300$ (inverse of ion cyclotron frequency).

Figure 4 shows the time evolution of power spectrum for the potentialenergy in k_z space defined by $E_\phi(k_z) = \sum_{k_x, k_y} |\phi_k|^2$. Time slices of t =100, 500, 1000, 1200, 1500 are shown. The convective cell mode glows and the normal cascade occurs in k_z space, simultaneously.

Figure 5 shows the time evolution of power spectrum for the potential energy defined by $E_\phi(k_x, k_y) = \sum_{k_z} |\phi_{\mathbf{k}}|^2$ in the case with $k_x = 0.15$. Time slice of t =100, 500, 1000,1200, 1500 are shown. The cascade and invers cascade occurs in k_y space and the spectrum tends to be flat at $t = 1500$ and the $k_y = 0$ mode is nonlinearly excited. Figure 6 shows the power spectrum of potential energy for convective cell mode defined by $E_\phi(k_x, k_y, k_z = 0) = |\phi_k|^2$ at $t = 1500$. The cases with $k_x = 0, \pm 0.15, \pm 0.30$ are plotted.The long dashed dotted line with diamonds indicates the mode with $k_x = 0$, the thick line with black circles, the mode with $k_x = 0.15$,the thick line with black squares, the mode with $k_x = 0.30$, the dashed line with circles, the mode with $k_x = -0.15$ and the dashed line with squares, the mode with $k_x = -0.30$. It is clearly seen that the components of zonal flow with $k_x = \pm 0.15, k_y = 0$ are dominant in the convective cell mode of potential energy.

Figure 7 shows the time evolution of energy for drift wave E_{DW} and convective cell mode E_{CC} in the case with $\nu_{ii} = 0.01$. It is found that the energy for convective cell mode is larger than that of the drift wave compared with the collisionless case. Fig. 8 shows the power spectrum of potential energy for convective cell mode $E_\phi(k_x, k_y, k_z = 0)$ at $t = 800$ in the case with $\nu_{ii} = 0.01$. It is seen that the zonal flow is damped by the collision, however, finite k_y modes with $k_x = \pm 0.30, k_y = \mp 0.15$ are excited instead. The amplitude of potential energy for drift wave is also larger than that obtained in the collisionless case.

Figure 9 shows the time evolution of energy for convective cell mode E_{CC} and particle flux defined by $\Gamma_{k=0} = \sum_{k=k'+k''} n_{k'}(-\mathrm{i}k_{y''}\phi_{k''})$ in cases with $\nu_{ii} = 0$ and

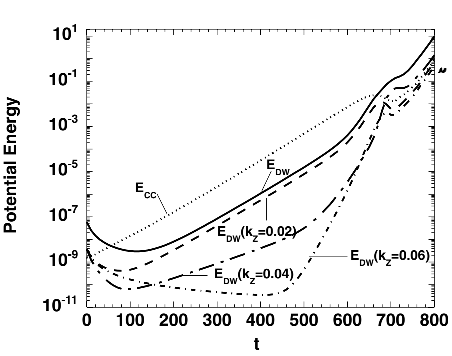

Fig. 7 Time evolution of energy for drift wave and convective cell modewith $\nu_{ii} = 0.01$.

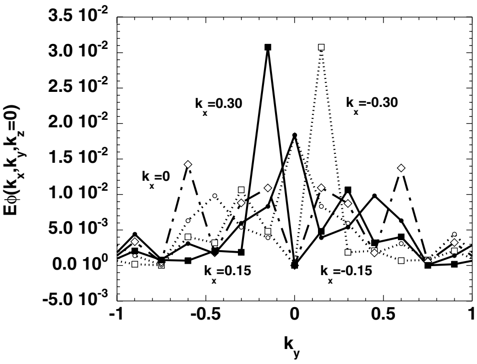

Fig. 8 Power spectrum of potential energy for convective cell mode $E_{\phi}(k_x, k_y, k_z = 0)$ with $\nu_{ii} = 0.01$ at $t = 800$.

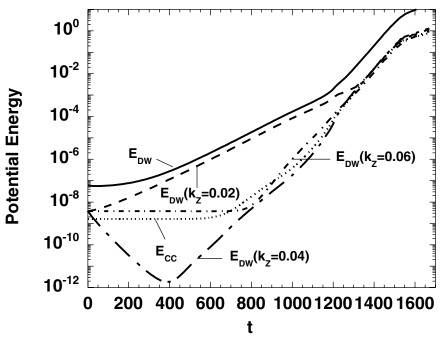

Fig. 9 Time evolution of energy of convective cell mode and flux.

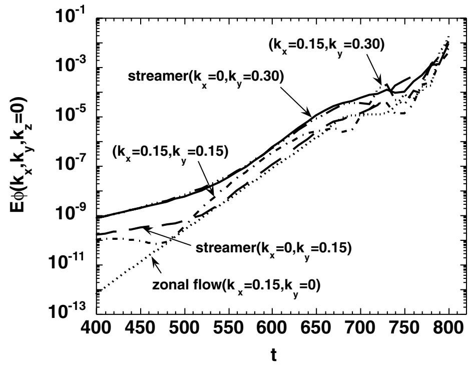

Fig. 10 Time evolution of power spectrum of potential energy for convective cell mode.

$\nu_{ii} = 0.01$. The thick lines represent the flux and the dashed lines, the energy of convective cell mode.In the case with $\nu_{ii} = 0.01$, the growth of flux is rapid compared with that obtained in the case without collision. It is found that flux and energy of convective cell mode correlates with each other for $E_{CC} \gg 10^{-2}$. Figure 10 shows the time evolution of power spectrum of energy for convective cell mode in the case with $\nu_{ii} = 0.01$. It is found that the component of streamer $k_x = 0.0, k_y = 0.3$ has the large contributionin convective cell mode. The contribution of the zonal flow $k_x = 0.15, k_y = 0.0$ is rather small. The electron nonlinearity excites various Fourier modes in convective cell mode, which affects the amplitude of drift wave turbulence as a back reaction, so that the simple picture such that the collisional damping of zonal flow determines the saturation level of drift wave turbulence might not be drawn for non-adiabatic electron response.

4. Conclusion

Nonlinear simulations of universal drift wave turbulence are performed by Kinetic-fluid model in the shearless slab geometry. The forward cascade is observed in k_z space and the forward/inverse cascade is observed in k_y space in the time evolution of energy spectrum.It is shown that the convective cell mode is nonlinearly excited similar to the zonal flow generation of ITG turbulence, however, no saturation is attained in these simulations. This is attributed from the fact that instability source exists in the short wavelength region of k_y space. For ITG turbulence, instability source exists in the longwavelength region and there is enough energy sink in the shortwavelength region. Therefore, we limit our discussion on the excitation of convective cell mode by the drift wave with $k_y \sim 1$ in the development of turbulence not on the statistical property of turbulence in the saturation phase. To attain the real saturation of universal drift wave turbulence, we should include the electron Lamor radius effect to stabilize universal drift wave in the short wave length region $k_y \gg 1$, which is missing in our model. In addition,we should extend the system size at least 10 times larger than that in this study to cover enough dissipation range (up to the Debye scale). Such a simulation with high resolution for k_y spectral space is gigantic and beyond the scope of this study. It should be investigated as a future work.The ion-ion collision effect on convective cell mode is also investigated. The ion-ion collision damps the zonal flow and instead excites streamer and finite k_y modes, which dominates the amplitude of convective cell mode. As the result, the flux is larger than that obtained in the case without collision.The electron nonlinearity excites various Fourier modes in convective cell mode, which affects the amplitude of drift wave turbulence as a back reaction, so that the simple pictures such that the collisional damping of zonal flow determines the saturation level of drift wave turbulence might not be drawn for the non-adiabatic electron case. It should be clearified the effect of the electron nonlineairy on the excitation of convective cell mode (including zonal flow, streamer, geodesic acoustic mode etc.) in toroidal geometry. It is also left as a future work.

References

[1] Z. Lin *et al*., Science **281**, 1835 (1998).
[2] P.H. Diamond *et al*., *Fusion Energy* 1998 (Proc. 17th Int. Conf. Yokohama, Japan, 1998) Vol.4, 1421.
[3] R.Z. Sagdeev, V.D. Shapiro and V.I. Shevchenko, Fiz. Plazmy **4**, 551 (May-June 1978).
[4] C.Z. Cheng and H. Okuda, Phys. Rev. Lett. **38**, 708 (1997).
[5] A.I. Smolyakov, P.H. Diamond and M. Malkov, Phys. Rev. Lett. **84**, 491(2000).
[6] F.L. Hinton *et al*., APS, 41st Annual Meeting of DPP, Seattle 1999 UP 166H.
[7] C.Z. Cheng and J.R. Johnson, J. Geophys. Res. **104**, 413 (1999).
[8] M. Yagi, C.Z. Cheng and T.S. Hahm, *Proc. of Symposium on 'Transport and Strctural Formation' combined with US/Japan JIFT workshop 'Strctural Formation and Drift/MHD Turbulence'*, Rep. of RIAM, Kyushu Univ., No.S-1,157 (2003).